DE GRUYTER
OPEN

X-ray diffraction and Mössbauer spectroscopy studies of a mechanosynthesized Fe$_{75}$B$_{25}$ alloy

Elżbieta Jartych,
Ludmila M. Kubalova,
Victoria I. Fadeeva

Abstract. In this work, the process of formation of metastable phases was investigated for the Fe$_{75}$B$_{25}$ composition. Mechanical synthesis was performed in a MAPF-2M high-energy planetary ball mill under an argon atmosphere. X-ray diffraction (XRD), differential scanning calorimetry (DSC), and Mössbauer spectroscopy (MS) were applied to recognize the phases. After 6 h of milling, the material consisted of two phases, that is, metastable tetragonal t-Fe$_2$B and amorphous phases. During further thermal processing, the metastable phase was transformed into the stable Fe$_2$B phase.

Key words: mechanosynthesis • metastable phase • Mössbauer spectroscopy • X-ray diffraction

E. Jartych✉
Institute of Electronics and Information Technology,
Lublin University of Technology,
38A Nadbystrzycka Str., 20-618 Lublin, Poland,
Tel.: +48 81 538 4618, Fax: +48 81 538 4312,
E-mail: e.jartych@pollub.pl

L. M. Kubalova
Department of Chemistry,
North Ossetian State University after K. L. Khetagurov,
44-46 Vatutina Str., 362025 Vladikavkaz, Russia

V. I. Fadeeva
Department of Chemistry,
M. V. Lomonosov Moscow State University,
Leninsky Gory, 119899 Moscow, Russia

Introduction

Mechanical synthesis of iron with p-elements (Al, Si, Ge, and B) often leads to the formation of metastable phases. Based on many works, it may be stated that the probability of formation of metastable phases during mechanical synthesis depends on the differences in atomic radii of constituents as well as electronegativity [1]. Recently, it was observed that for near-equiatomic composition of Fe-X$_p$ alloys (X$_p$: Al, Si, Ge, and B) the formation of solid solutions, silicides, germanides and borides depends on the strength of covalent bonding of the p-element [2]. In the case of a metal–metal system with free electrons, that is, Fe-Al alloys, disordered solid solutions are mainly formed. Mechanical synthesis of Fe with semimetals (Si and Ge) with a high level of covalence leads to the formation of the ordered phases, that is, FeSi, FeGe$_2$, β-Fe$_5$Ge$_3$ and FeGe [2].

In this work, the process of formation of metastable phases was investigated for Fe$_{75}$B$_{25}$, that is, a metal–nonmetal system, where B has covalent bonding. X-ray diffraction (XRD), calorimetry and Mössbauer spectroscopy studies were used as complementary methods in order to obtain information about structure, thermal stability and hyperfine interaction parameters of the material.

Experimental details

Powders of iron (purity: 99.9%) and amorphous boron (purity: 99.88%) were mixed in suitable

proportions to obtain the $Fe_{75}B_{25}$ composition. Mechanical synthesis was performed in a water-cooled high-energy planetary ball mill of the type MAPF-2M under an argon atmosphere. Stainless steel balls were used, the ball-to-powder weight ratio was 6:1, and the total mass of the mixture was 9 g. The energy consumption during milling of ~10 W/g caused the increase in the temperature up to 80–230°C; hence, the cycle of work was interrupted every 3 min.

The samples were examined using XRD (DRON--4-07 system, CuK_α radiation) and differential scanning calorimetry (DSC; NTZSCH STA). The DSC measurements were carried out under heating in a helium atmosphere at the rate of 20 K per min. Mössbauer spectroscopy measurements were performed at room temperature in transmission geometry using a source of ^{57}Co in a rhodium matrix. The chemical composition of the sample after 6 h of milling was determined by means of a Camebax--Microbeam microanalyzer in a scanning mode using the characteristic spectra of K-series of Fe.

Results and discussion

During milling, systematic fragmentation of powders occurs, which leads to broadening of diffraction lines (Fig. 1). In every sample, after 0.5, 1 and 2 h of milling times, iron is present as a crystalline phase (the most intensive diffraction line near 44° is visible in all the patterns). The arrangement of Bragg peaks changes after 2 h of milling, and patterns registered after 4, 5 and 6 h have practically the same shape. After six hours of milling, alloy composition changes and becomes $Fe_{78.8}B_{21.2}$. The increase of Fe content in the obtained powder is due to abrasion of the steel balls and the mill container. At the same time, the loss of boron in the sample may be due to sublimation of boron from the surface of the grains during the milling process and local increase of temperature (this effect was observed for a Fe-B system and reported in Ref. [3]). The detailed analysis of the XRD pattern of the sample milled for 6 h (Fig. 2) revealed the existence of two phases, namely, an amorphous phase and the metastable tetragonal t-Fe_2B phase.

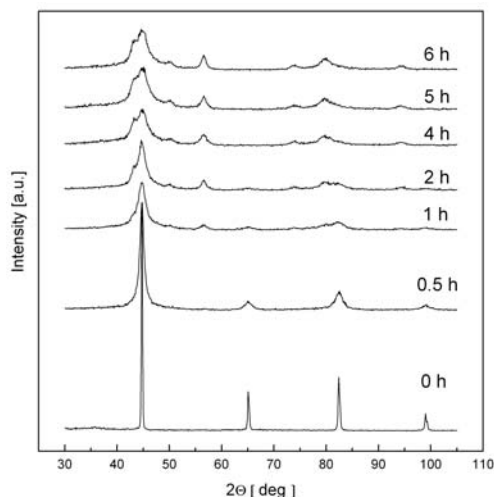**Fig. 1.** XRD patterns of $Fe_{75}B_{25}$ after various milling times.

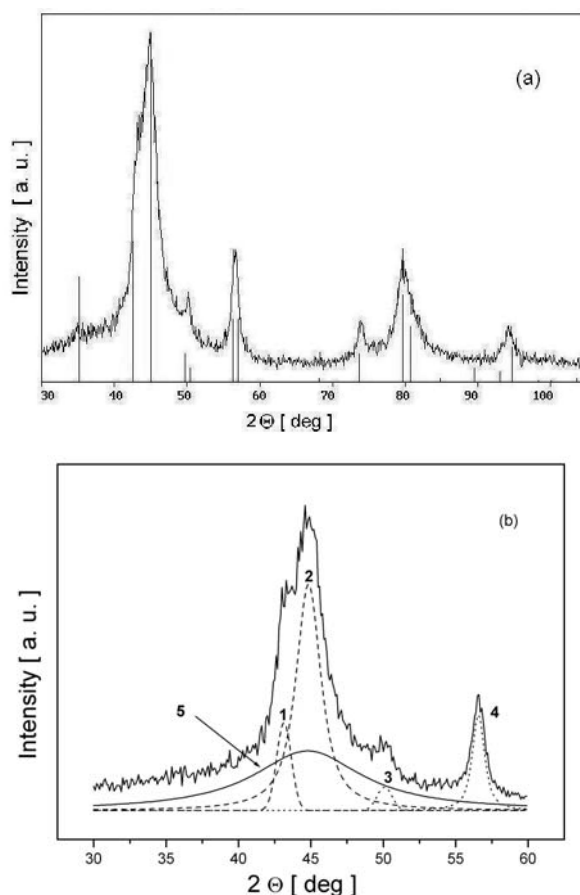**Fig. 2.** (a) XRD pattern of $Fe_{75}B_{25}$ after 6 h of milling; positions of lines for the tetragonal t-Fe_2B phase are marked according to JCPDS card-file No 39-1314; (b) deconvolution of the main peaks of $Fe_{75}B_{25}$ after 6 h of milling; peaks numbers 1–4 are from the t-Fe_2B phase, and peak 5 is from the amorphous phase.

In Fig. 2a, the angular positions of diffraction lines agree well with the database for the metastable tetragonal t-Fe_2B phase (JCPDS card-file No. 39--1314). The average crystallite size of the t-Fe_2B phase estimated from the broadening of diffraction lines is $D \sim 10$ nm. The determined values of the lattice parameters are as follows: $a = 0.5130$ nm and $c = 0.8532$ nm. They are different, especially the c value, in comparison with the parameters for the stable Fe_2B phase $C16$ (see Table 1). Deconvolution of the XRD pattern (Fig. 2b) allowed us to determine the phase relationship. The relative contribution is 53% for the metastable t-Fe_2B phase and 47% for the amorphous phase.

A calorimetric study was performed to get information about the thermal stability of the material (Fig. 3). The exothermic peak in the DSC curve corresponds to the crystallization of the amorphous phase. Moreover, a weak endothermic effect in the DSC curve in the temperature range of 800–850°C may be observed. It can be associated with the transition of metastable phases into the stable state, which requires a supply of the thermal energy. Transition to the equilibrium state takes place as a result of heating up to 1000°C.

From the DSC curve, the heating temperatures were chosen for subsequent thermal processing of

Table 1. Structural data for the phases obtained after heating up to 1000°C of a $Fe_{75}B_{25}$ alloy milled for 6 h

	α-Fe	Fe_2B ($C16$)
Lattice parameter	a = 0.2866 nm	a = 0.5107 nm; c = 0.4241 nm
Coherent scattering domain	D = 46 nm	D = 60 nm
Medium lattice microstrain	ε = 0.101%	ε = 0.027%
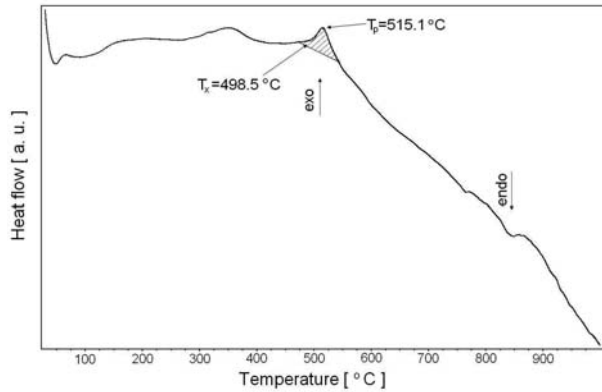
Fig. 3. DSC curve of $Fe_{75}B_{25}$ after 6 h of milling; T_x – onset crystallization temperature and T_p – peak temperature.

the material. Results of XRD studies on the samples heated in the calorimeter up to various temperatures are shown in Fig. 4. Depending on the rate of sample heating, characteristic temperatures can be shifted. After heating up to 440°C, in the XRD pattern, there is no amorphous halo; lines from α-Fe and some nanocrystalline Fe_2B phase (metastable) appear. The weak lines of the metastable cubic $Fe_{23}B_6$ – τ-phase and the lines of the Fe_2B phase appear in the diffraction pattern of the alloy after heating up to 650°C. Lines of the τ-phase have very low intensity and are indicated by arrows in the diffraction pattern (Fig. 4). After heating up to 1000°C, the alloy contains α-Fe and the stable tetragonal Fe_2B phase ($C16$ type). A characteristic feature of the transformation from the metastable Fe_2B to a stable phase is observed in the range of 2Θ angle from 54° to 60° (see enlarged patterns in Fig. 4). The splitting of
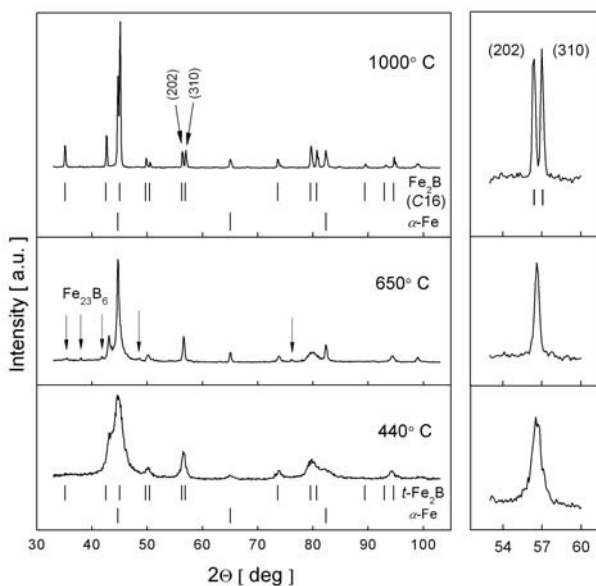
the line of the metastable phase does not occur (for 440°C and 650°C). Reflections indexed by (204) and (105) merge into one line for which the interplanar distance d = 0.1625 nm. The line of the stable Fe_2B phase with the $C16$ structure is split into two: (202) with d = 0.1634 nm and (310) with d = 0.1615 nm. This splitting is clearly observed in the diffraction pattern of the sample after heating up to 1000°C. The lattice parameters of phases recognized in the material after the thermal process are listed in Table 1 together with other structural data.

Mössbauer spectroscopy measurements performed for the samples milled for 4 and 6 h revealed the same shape of the spectra, which were the superposition of two sextets (Fig. 5). Hyperfine interaction parameters determined from the fitting of each spectrum are listed in Table 2. The first sextet comes from α-iron; however, the value of the hyperfine magnetic field for this component is slightly increased as compared to the value for an ordinary α-iron (33.0 T). It is known from the literature that in the iron subjected to ball milling, the reduction of grain sizes occurs down to the nanometer level. This leads to the broadening of the spectral lines as well as to the increase of the hyperfine magnetic field [4, 5]. Hence, this component was named nano-Fe and may be hidden inside the amorphous halo seen in the XRD pattern. The relative contribution of the nano-Fe phase determined from the area of the Mössbauer spectrum is about 5%. The second sextet may be attributed to the metastable t-Fe_2B phase. The values of hyperfine interaction parameters agree well with literature data [6, 7]. The significant broadening of spectral lines ($\Gamma_{1,2,3}$ in Table 2) testifies the fragmentation of the structure down to the nanometer level.
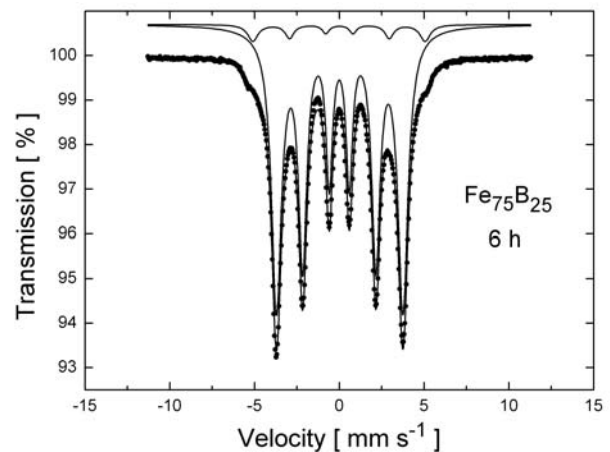

Fig. 4. XRD patterns of $Fe_{75}B_{25}$ after 6 h of milling and thermal treatment.

Fig. 5. Room-temperature Mössbauer spectrum of $Fe_{75}B_{25}$ after 6 h of milling.

Table 2. Hyperfine interaction parameters for $Fe_{75}B_{25}$ after 4 and 6 h of milling. δ – Isomer shift relative to α-iron; Δ – quadrupole shift; B_{hf} – hyperfine magnetic field; $\Gamma_{1,2,3}$ – half width at half maximum of spectral lines no. 1, 2 and 3, respectively; uncertainty of the δ, Δ and $\Gamma_{1,2,3}$ parameters is 0.01 mm·s^{-1}, 0.02 T for B_{hf}

Milling time [h]	δ [mm·s^{-1}]	Δ [mm·s^{-1}]	B_{hf} [T]	$\Gamma_{1,2,3}$ [mm·s^{-1}]	Component
4	0.02	−0.07	33.77	0.34; 0.35; 0.27	Nano-Fe
	0.11	0.02	22.89	0.34; 0.35; 0.27	t-Fe$_2$B
6	0.08	−0.02	33.25	0.36; 0.30; 0.23	Nano-Fe
	0.11	0.02	23.22	0.36; 0.30; 0.23	t-Fe$_2$B

Conclusions

The process of formation of phases during mechanosynthesis and subsequent thermal treatment of $Fe_{75}B_{25}$ was monitored by XRD, differential scanning calorimetry and Mössbauer spectroscopy. It was shown that during mechanical synthesis of $Fe_{75}B_{25}$, the nanocrystalline metastable t-Fe$_2$B phase was formed together with an amorphous phase. Mössbauer spectroscopy studies also revealed a small amount of nanocrystalline α-iron. The metastable t-Fe$_2$B phase coexists with the nano/amorphous phase in the relatively broad range of temperatures. During heating up to 650°C, a small amount of the $Fe_{23}B_6$ – τ-phase could be transformed from the amorphous phase. An elevated heating temperature, that is, 1000°C, allowed the metastable t-Fe$_2$B phase to transform into the stable $C16$ phase.

References

1. Bansal, C., Gao, Z. -Q., Hong, L. B., & Fultz, B. (1994). Phases and phase stabilities of Fe$_3$ X alloys (X=Al, As, Ge, In, Sb, Si, Sn, Zn) prepared by mechanical alloying. *J. Appl. Phys.*, *76*, 5961–5966. DOI: 10.1063/1.358375.

2. Kubalova, L. M., & Fadeeva, V. I. (2014). Struktura mechanosyntezirovannych splavov zheleza s p-elementami (Ai, Si, Ge, B) ekvatomnogo sostava. *Izviestia RAN. Seria Fizicheskaya*, *78*, 131–134. DOI: 10.7868/S0367676513090251.

3. Ackermann, M., Wagner, H. -G., Gonser, U., & Steiner, P. (1986). Bulk and surface crystallization behavior of Fe$_{100-x}$B$_x$. *Hyperfine Interact.*, *27*, 397–400. DOI: 10.1007/BF02354790.

4. Schaaf, P., Rixecker, G., Yang, E., Wagner, C. N. J., & Gonser, U. (1994). Study on nanocrystalline and amorphous powders prepared by mechanical alloying. *Hyperfine Interact.*, *94*, 2239–2244. DOI: 10.1007/BF02063769.

5. Del Bianco, L., Hernando, A., Bonetti, E., & Navarro, E. (1997). Grain-boundary structure and magnetic behavior in nanocrystalline ball-milled iron. *Phys. Rev. B*, *56*, 8894–8901. DOI: 10.1103/PhysRevB.56.8894.

6. Sanchez, F. H., Budnick, J. I., Zhang, Y. D., Hines, W. A., Choi, M., & Hasegawa, R. (1986). Mössbauer study of the local atomic environments in metastable crystalline Fe-B alloys. *Phys. Rev. B*, *34*, 4738. DOI: 10.1103/PhysRevB.34.4738.

7. Fernández van Raap, M. B., Sánchez, F. H., & Zhang, Y. D. (1995). On the microstructure and thermal stability of rapidly quenched Fe-B alloys in the intermediate composition range between the crystalline and amorphous states. *J. Mater. Res.*, *10*, 1919–1926. DOI: 10.1557/JMR.1995.1917.